AD NUMBER
AD018796
CLASSIFICATION CHANGES
TO: **unclassified**
FROM: **confidential**
LIMITATION CHANGES
TO: **Approved for public release; distribution is unlimited.**
FROM: **Distribution authorized to U.S. Gov't. agencies and their contractors; Administrative/Operational Use; 28 APR 1953. Other requests shall be referred to Naval Ordnance Systems Command, Washington, DC.**
AUTHORITY
30 apr 1965, DoDD 5200.10; usnol ltr, 29 aug 1974

AD _____

NAVORD REPORT 2823

MEASUREMENTS OF PRESSURE DISTRIBUTION AND BOUNDARY-LAYER TRANSITION ON A HOLLOW-CYLINDER MODEL

28 APRIL 1953

U. S. NAVAL ORDNANCE LABORATORY
WHITE OAK, MARYLAND

UNCLASSIFIED
NAVORD Report 2823

Aeroballistic Research Report 176

MEASUREMENTS OF PRESSURE DISTRIBUTION AND BOUNDARY-LAYER TRANSITION ON A HOLLOW-CYLINDER MODEL

By

Roland E. Lee

ABSTRACT: Static pressure distributions and location of boundary-layer transition were determined on a 4" outer diameter hollow-cylinder model. Its centerline was adjusted parallel to the flow in the NOL 40 x 40 cm Aeroballistics Intermittent Wind Tunnel No. 2 at six Mach numbers between 2.2 and 5.0. At these Mach numbers the normal shock wave was "swallowed" by the cylinder, i.e., supersonic flow was attained inside the cylinder. Pressure distributions on the hollow cylinder were found to be nearly the same as the free-stream static pressure distribution. The location of boundary-layer transition was determined from schlieren photographs. It was found that the transition Reynolds numbers for the hollow cylinder decreased with increasing Mach number. The results of the boundary-layer transition were compared with those obtained previously on a 5° cone and a 20° cone-cylinder in the same tunnel.

U. S. NAVAL ORDNANCE LABORATORY
WHITE OAK, MARYLAND

NAVORD Report 2823 28 April 1953

This report contains information on pressure distributions and boundary-layer transition on the outer surface of a hollow-cylinder model.

The work was initiated as a feasibility study for the use of such models for experimental investigations of local skin-friction drag with laminar and turbulent boundary-layer flow in the NOL 40 x 40 cm Aeroballistics Wind Tunnel No. 2 during the year 1952. The use of the hollow cylinder as a model for skin-friction investigations had been proposed by J. L. Potter now with Redstone Arsenal.

The project has been sponsored jointly by the U. S. Bureau of Ordnance under Task No. Re9a-108 and the Office of Naval Research under Task No. NR-061-069.

The author wishes to acknowledge the work contributed by F. Geineder and R. T. Schroth in the design of the hollow-cylinder model and the technical comment, criticism and support of R. Lehnert and S. M. Hastings.

E. L. WOODYARD
Captain, USN
Commander

H. H. KURZWEG, Chief
Aeroballistic Research Department
By direction

CONTENTS

ILLUSTRATIONS

MEASUREMENTS OF PRESSURE DISTRIBUTION AND BOUNDARY-LAYER TRANSITION ON A HOLLOW-CYLINDER MODEL

I. INTRODUCTION

1. This investigation is the first of a series of feasibility studies aimed at the direct measurement of local laminar and turbulent skin-friction drag, boundary-layer profiles, recovery temperatures and heat-transfer characteristics on a model without pressure gradient. The conventional flat plate is replaced by a hollow cylinder, i.e., a "wrapped" flat plate, having its axis parallel with the flow. The flow over the cylinder would not be subject to flow contamination due to side-wall effects as encountered with flat plate models. The flow over the hollow cylinder can be correlated to flows over bodies of revolution such as cone-cylinders and ogive-cylinders which are of practical importance in the design of missiles.

2. The purpose of the present investigation is to measure the pressure distribution along the outer surface of the hollow cylinder in order to determine the suitability of such models as well as to measure the location of the boundary-layer transition from the leading edge of the cylinder over the range of Mach numbers available in the NOL 40 x 40 cm Wind Tunnel. From the result of this investigation we can select the proper location for measuring local skin-friction drag, etc., in the laminar or turbulent region.

II. EQUIPMENT AND EXPERIMENTAL METHODS

3. All experimental work is performed in the NOL 40 x 40 cm Aeroballistics Intermittent Wind Tunnel No. 2 described in reference (a). This is an intermittent-flow tunnel with near atmospheric stagnation conditions. Six supersonic nozzles are used, giving an average Mach number over the model of M = 2.15, 2.47, 2.86, 3.25, 4.28 and 5.01. The normal shock wave is swallowed by the cylinder at these Mach numbers, i.e., supersonic flow is attained inside the cylinder. Reynolds numbers from 1 to 6 million, based on free-stream condition and cylinder length, are covered in this Mach number range.

The highest Mach number is associated with the lowest Reynolds number due to the fixed supply conditions of this tunnel.

4. The model, shown in Figure 1, was a hollow cylinder of 4" outer diameter with .062" wall thickness, 10° leading wedge angle and a 19" effective length made from a brass tube. A second similar tube was made with an effective length of 32" for boundary-layer transition investigation at the high Mach numbers. The model was mounted on a steel cylindrical base section 9½" in length with four 2" x 4½" openings to prevent choking, and a central hollow cylindrical sting. Two pairs of ½" diameter holes, 90° apart, through the base section, were used as supports for a roll angle adjustment rod. Eleven static pressure taps were located at 1, 3, 5, 7, 9, 11, 13, 15, 17, 18 and 18½ inches from the leading edge of the cylinder. For reasons of symmetry, four additional taps were placed on the opposite outer surface of the cylinder at 1, 9, 18 and 18 1/2 inches from the leading edge. The tubings connected to the pressure taps were led out through the hollow sting. Stainless steel tubings having .042" inner diameter were used for 5 of the 6 Mach numbers tested but were found to be too small to obtain pressure equilibrium at M = 5.01 within the blowing time which is approximately 35 seconds. At this Mach number .080" i.d. copper tubings were used. Due to the large over-all length of the model, special care was taken to mount the model within the test rhombus at each Mach number. In each case the final adjustment of the model in the test section was within 5 minutes of the required angle of attack, $\alpha = 0^{\circ}$, and the desired roll angle, θ. The model length limited the range of Mach numbers tested to nozzles above M = 2 since the length of the test rhombus decreased with decreasing Mach number.

5. No special effort was made to achieve an exceptionally smooth surface. Surface roughness was measured by a Brush profilometer, Model-BL 103, on 13 selected sections of the cylinder. The roughness, indicated between peak and valley of the surface, was 68 microinches averaged over the 13 measurements. Since the brass cylinder was made from a tube section whose composition was not as homogeneous as one would desire, and small impure particles were seen scattered throughout

the metal, this average was not a true representation of the roughness on the surface of the hollow cylinder.

6. Pressure measurements were made with two 0-100 mm of mercury absolute Statham gauges at $\overline{M}$ = 2.15, 2.47, 2.86 and two 0-25 mm of mercury absolute Statham gauges at $\overline{M}$ = 3.25. The Statham gauges were used in combination with a two channel strain gauge indicator employing the "null" system of indication operated at a frequency of 400 cycles per second. A detailed description of this instrument is found in reference (a). The accuracy of these Statham gauges, claimed by the manufacturer, is within 1% of full scale reading. At Mach numbers of $\overline{M}$ = 4.28 and 5.01, the pressure distribution was measured with a fluid manometer bank designed by J. M. Kendall of NOL for the intermittent tunnels. A detailed description of this apparatus is presented in reference (b). Alkazene with a density of 1.739 g/cm^3 was used as the manometer fluid. With this fluid and the manometer bank, an accuracy of about 1% at a pressure of 1 mm of mercury was obtained.

7. Boundary-layer transition from laminar to turbulent flow was determined by the schlieren method. Spark-schlieren photographs were taken with a one microsecond exposure at an average rate of four pictures per blow. Figures 4 and 5 show samples of typical schlieren photographs of boundary-layer transition in each of the 6 nozzles tested. The distance from the transition point to the leading edge of the cylinder was measured directly on the negatives with a David W. Mann comparator, Model 6363, capable of reading distances to .01 mm.

8. The influence on transition caused by the presence of pressure taps on the model was determined by first measuring the location of transition directly above the pressure taps, i.e., the taps were at the point of tangency between the model surface and the schlieren beam, and secondly, rotating the cylinder model 90°, measuring the location of transition on the surface without pressure taps and comparing the two. An earlier transition was found when measured directly above the pressure taps. The results are plotted in Figure 7.

III. RESULT

9. The ratio of static pressure along the cylinder surface, p, to supply pressure of the tunnel, p_o, at the

various Mach numbers is presented in Figure 5. This ratio is compared with the free-stream static pressure distribution ratio p_s/p_o as obtained from tunnel calibrations. Each point on the graph represents an average of at least two independent measurements where the difference between the two is less than 1%. The increase in pressure at the last two stations is due to the shock wave formed around the base section which causes boundary-layer separation ahead of the shoulder. The flow around the shoulder can be seen in Figure 4 at three Mach numbers.

10. The pressure data are reduced further to pressure coefficients expressed in $\Delta p/p_s$ where Δp is equal to the measured local static pressure, p, minus the local free-stream static pressure, p_s. Figure 6 is a graph of the pressure coefficients at each Mach number vs. pressure tap locations. Table I shows the average pressure coefficient over the length of the model at each of the six Mach numbers. Also listed in the table is the average difference between corresponding upper and lower taps expressed in absolute values and in per cent. A check of the pressure distribution was made by rotating the model about its axis by 90° at $\bar{M} = 2.15$. The difference in pressure reading due to the rotation was found to be less than 1%.

TABLE I

$\bar{M}$	Average $\Delta p/p_s$	Pressure difference between corresponding upper and lower taps	
		mm of Hg	per cent
2.15	1 4%	1.77	2.3%
2.47	2.1%	.09	.2%
2.86	1.7%	.82	3.2%
3.25	2.2%	.44	3.1%
4.28	19.5%	.56	16.0%
5.01	30.7%	.35	24.9%

These average per cent deviations are based on the absolute pressure measured at each Mach number. Therefore, with a constant absolute pressure difference, one would expect a greater per cent deviation at the higher Mach numbers due to the decrease in the test chamber pressure. It should be noted that the static pressures

measured on the cylinder surface were 2" above and below the centerline while those of the calibrations were measured directly along the centerline.

11. The evaluation of schlieren photographs taken during individual blows indicated a fluctuation of the location of transition with respect to time. Figure 7 is a plot of the range of the fluctuation together with the average transition distance from the leading edge in each of the six nozzles. Each average point represents the mean location on the top and the bottom of the model as obtained from six or more schlieren photographs. Two sets of schlieren photographs of the transition were taken at the lower Mach numbers; one of the flow directly above the pressure taps and the other with the flow over a portion of the cylinder without pressure taps. It was found that the influence of pressure taps on the boundary layer decreased the transition Reynolds number by half a million.

12. A comparison of the transition Reynolds number of the hollow cylinder with the transition Reynolds number of a 20° cone-cylinder (reference c) and a 5° cone (reference d) measured in the same tunnel as a function of Mach number is presented in Figure 8. Transition Reynolds number is based on the wetted length of the model and free-stream conditions in all cases. The points shown on the graph are averages of 15 or more values measured on the hollow cylinder. The data from the hollow cylinder follow the trend of the cone and cone-cylinder rather well at higher Mach numbers but they follow the trend of the cone rather than the cone-cylinder at the low Mach numbers. This is remarkable because no pressure gradient exists along the hollow cylinder and the cone, whereas it is to be expected that the expansion around the shoulder and the pressure gradient along the adjacent cylinder influences the boundary layer of the cone-cylinder model.

IV. CONCLUSION

13. The following conclusion may be drawn from the result of the feasibility study with a hollow-cylinder model in the range of Mach numbers investigated.

a. The static pressure distribution on the outer surface of a hollow-cylinder model

is nearly the same as the static pressure distribution of the free-stream in the supersonic nozzle.

b. The boundary layer on the hollow-cylinder model is completely laminar at distances less than 6 inches from the leading edge of the cylinder and completely turbulent at distances greater than 20 inches from the leading edge in the range of Mach numbers tested, in the NOL 40 x 40 cm Aeroballistics Intermittent Wind Tunnel No. 2.

c. Pressure tap influence causes a decrease in transition Reynolds number up to a maximum of about half a million.

d. Region of trarsition oscillates within two extreme positions representing a difference in Reynolds number of one million.

e. Transition Reynolds number of the hollow cylinder as a function of Mach number follows the same trend as found on the cone and the cone-cylinder at higher Mach numbers tested in the same tunnel, i.e., transition Reynolds number decreases with increasing Mach number.

f. Since no notable pressure gradient is detected on the surface of the hollow cylinder, such a model would be suitable for studying boundary-layer profiles, skin friction, recovery temperature, etc, for flows without pressure gradient in the axial direction.

V. SYMBOLS

p	=	measured pressure
p_o	=	supply pressure
p_s	=	free-stream pressure
Δp	=	$p - p_s$
M	=	Mach number
$\bar{M}$	=	average Mach number over the model
Re_{trans}	=	transition Reynolds number
α	=	pitch angle
θ	=	roll angle

VI. REFERENCES

(a) Lightfoot, J. R., "The Naval Ordnance Laboratory Aeroballistic Research Facility", NOLR Report 1079, 15 August 1950, RESTRICTED.

(b) Kendall, J. M., "Equipment and Techniques for Making Pressure Measurements in Supersonic Wind Tunnels in Mach Numbers Up to 5", NAVORD Report 2580, 11 August 1952.

(c) Potter, J. L., "New Experimental Investigations of Friction Drag and Boundary-Layer Transition on Bodies of Revolution at Supersonic Speeds", NAVORD Report 2371, 24 April 1952.

(d) Lange, A. H. and Gieseler, P.L., "Measurement of Boundary-Layer Transition to Determine the Relative Disturbance Level in Two NOL Supersonic Wind Tunnels", NAVORD Report 2752.

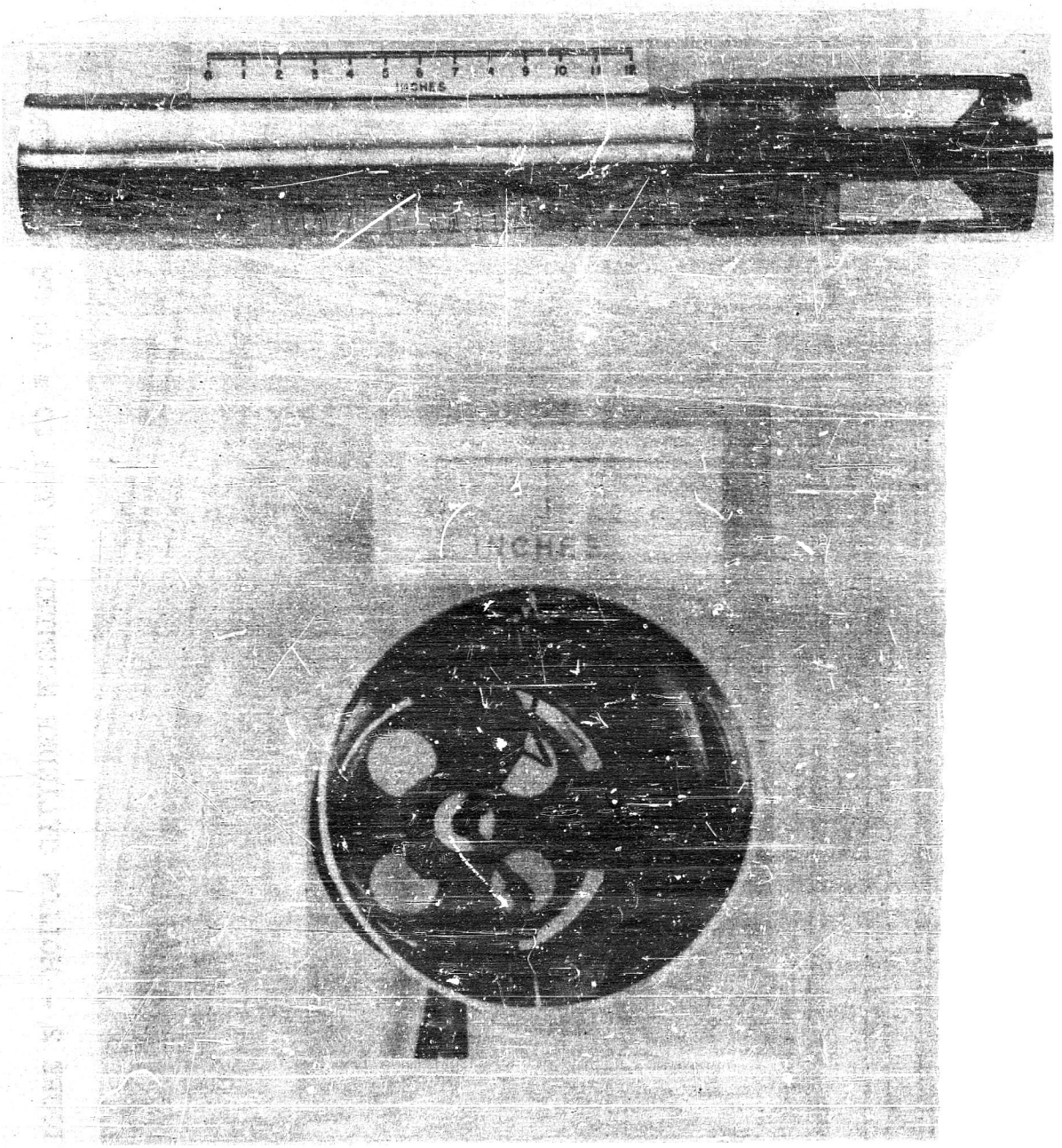

FIGURE 1 - FRONT AND SIDE VIEWS OF HOLLOW CYLINDER SHOWING PRESSURE TAP ARRANGEMENT

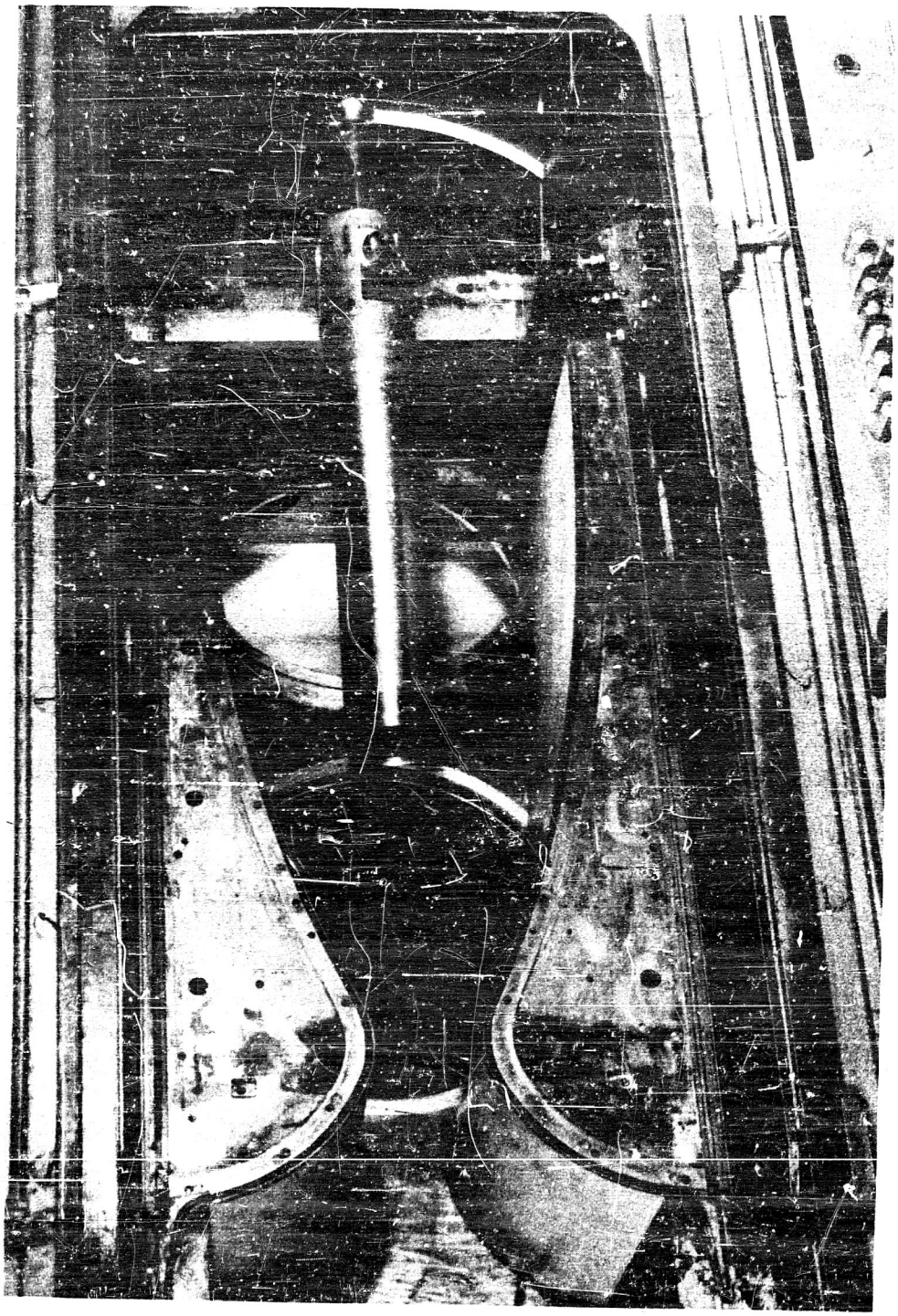

FIGURE 2 - HOLLOW CYLINDER MOUNTED IN THE 40 x 40 CM WIND TUNNEL

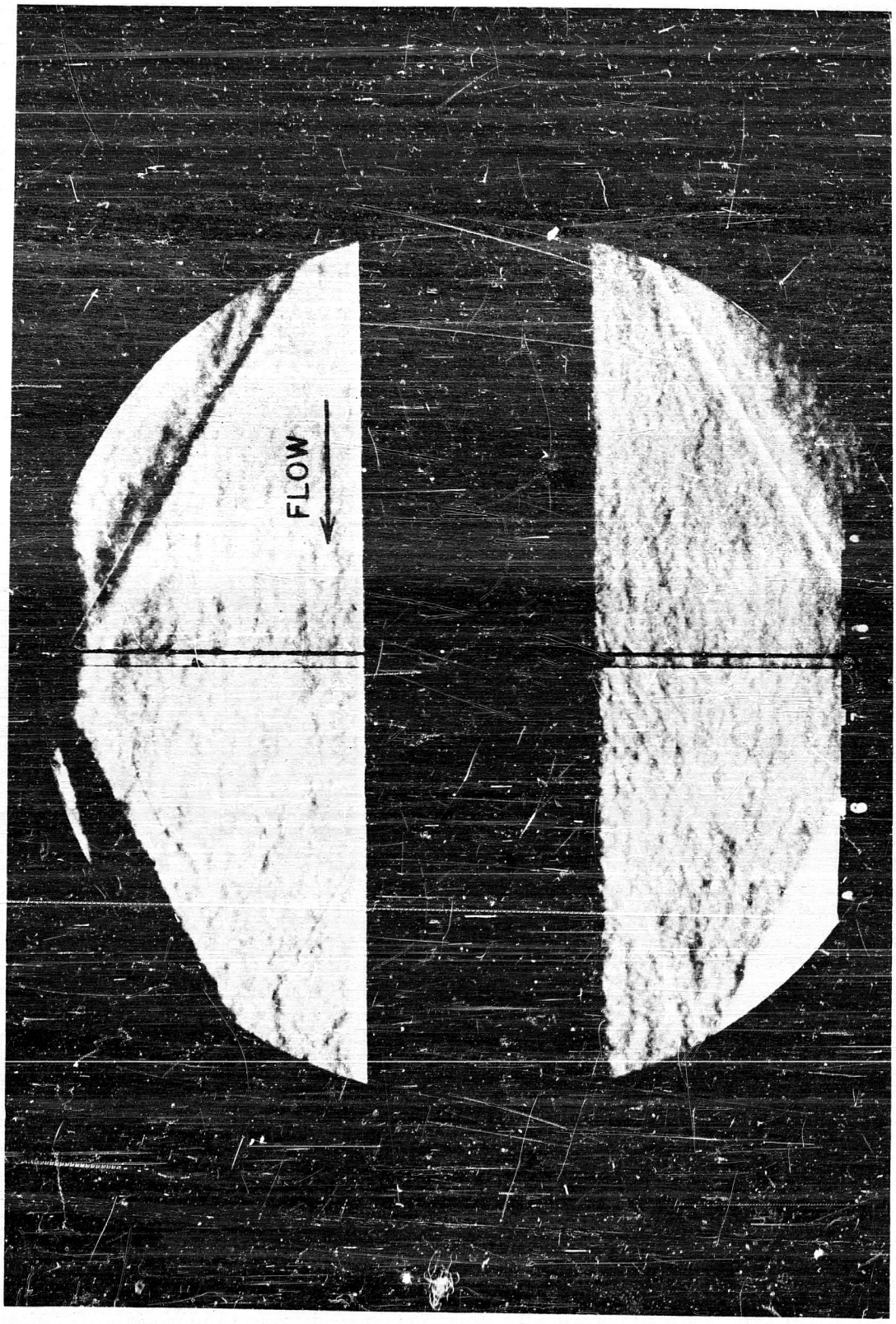

FIGURE 3 - SCHLIEREN PHOTOGRAPH OF HOLLOW CYLINDER (M = 2.15)

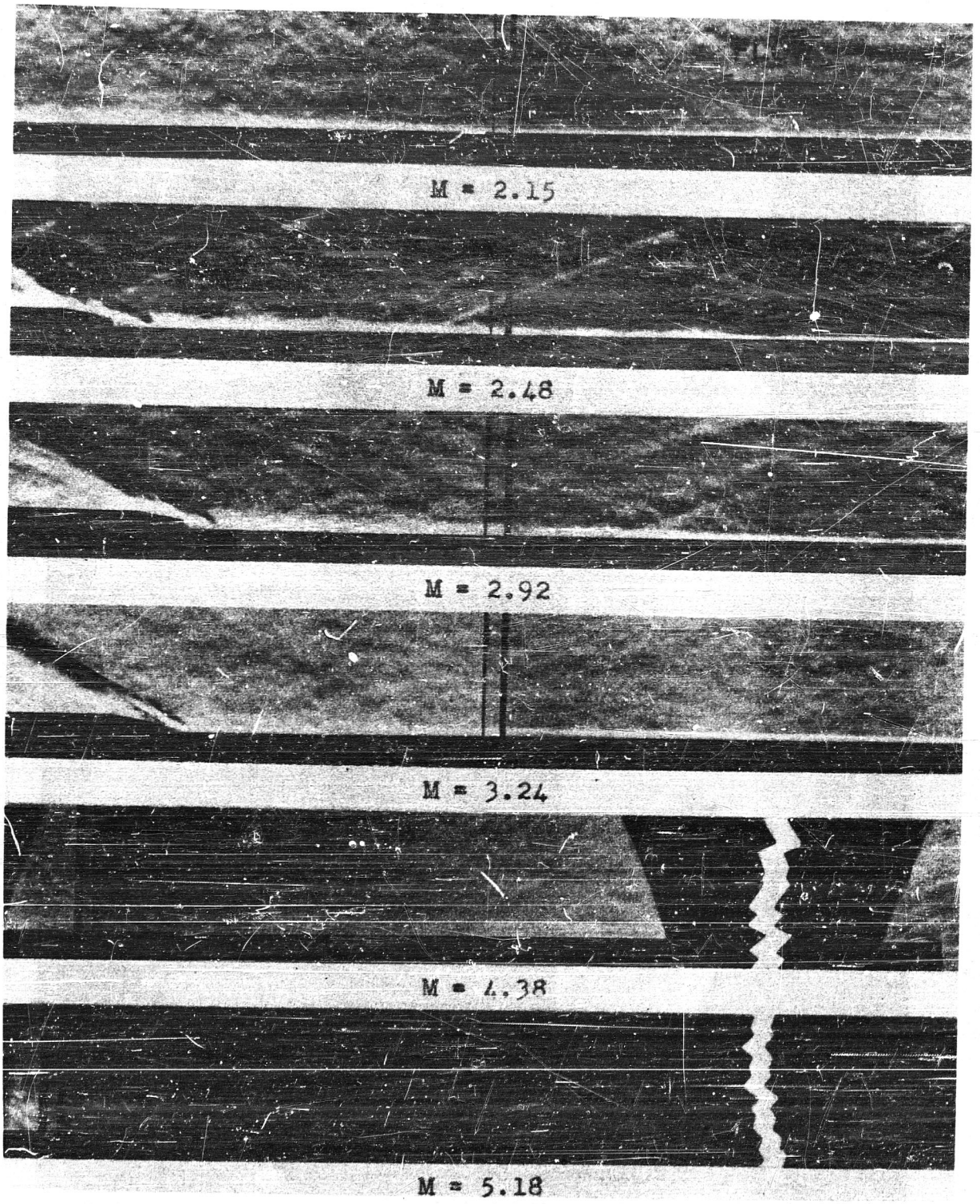

FIGURE 4 - SCHLIEREN PHOTOGRAPHS OF BOUNDARY LAYER ON HOLLOW CYLINDER

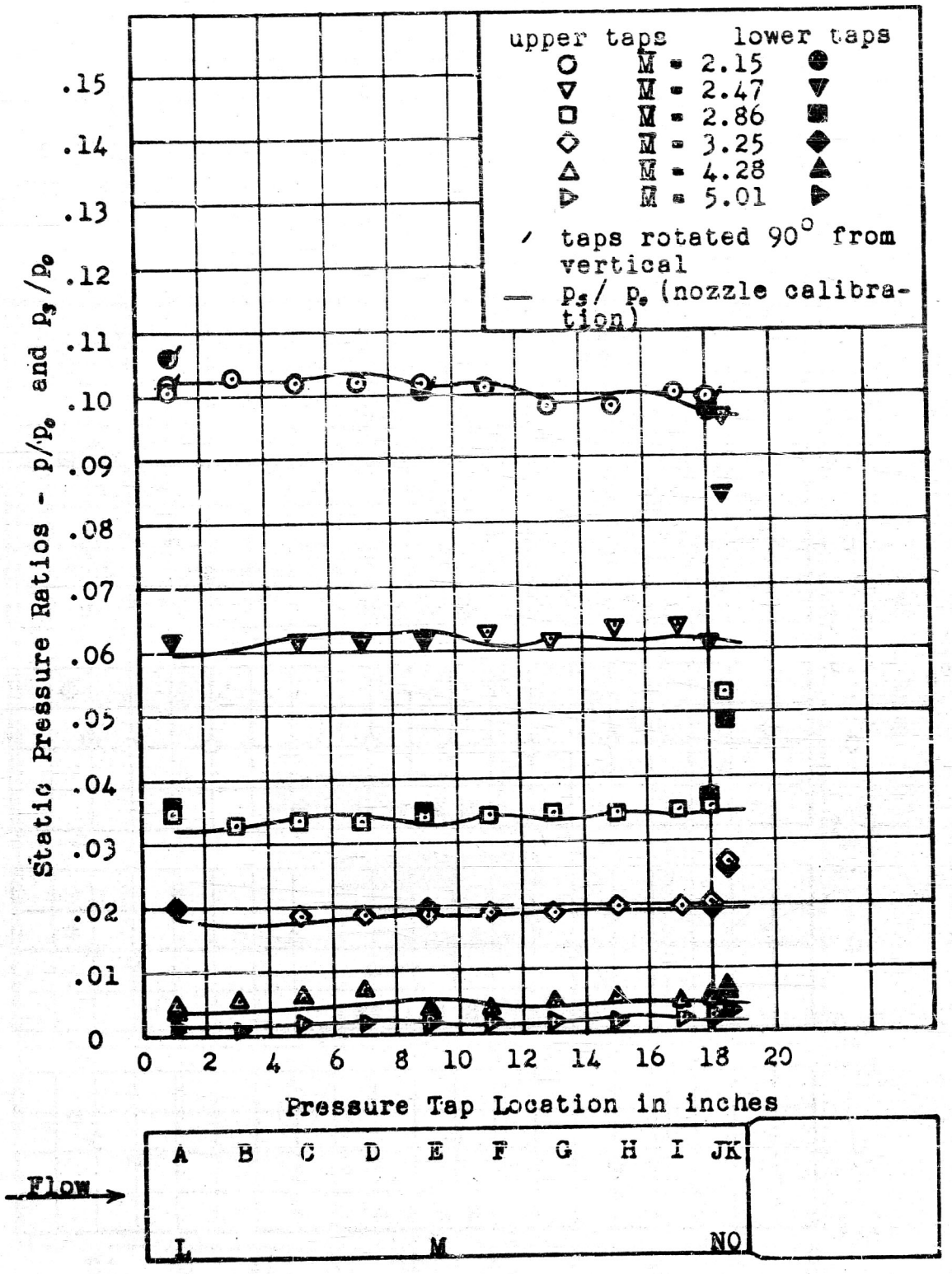

FIGURE 5 - PRESSURE DISTRIBUTION ON HOLLOW CYLINDER COMPARED WITH NOZZLE CALIBRATION ALONG THE CENTERLINE

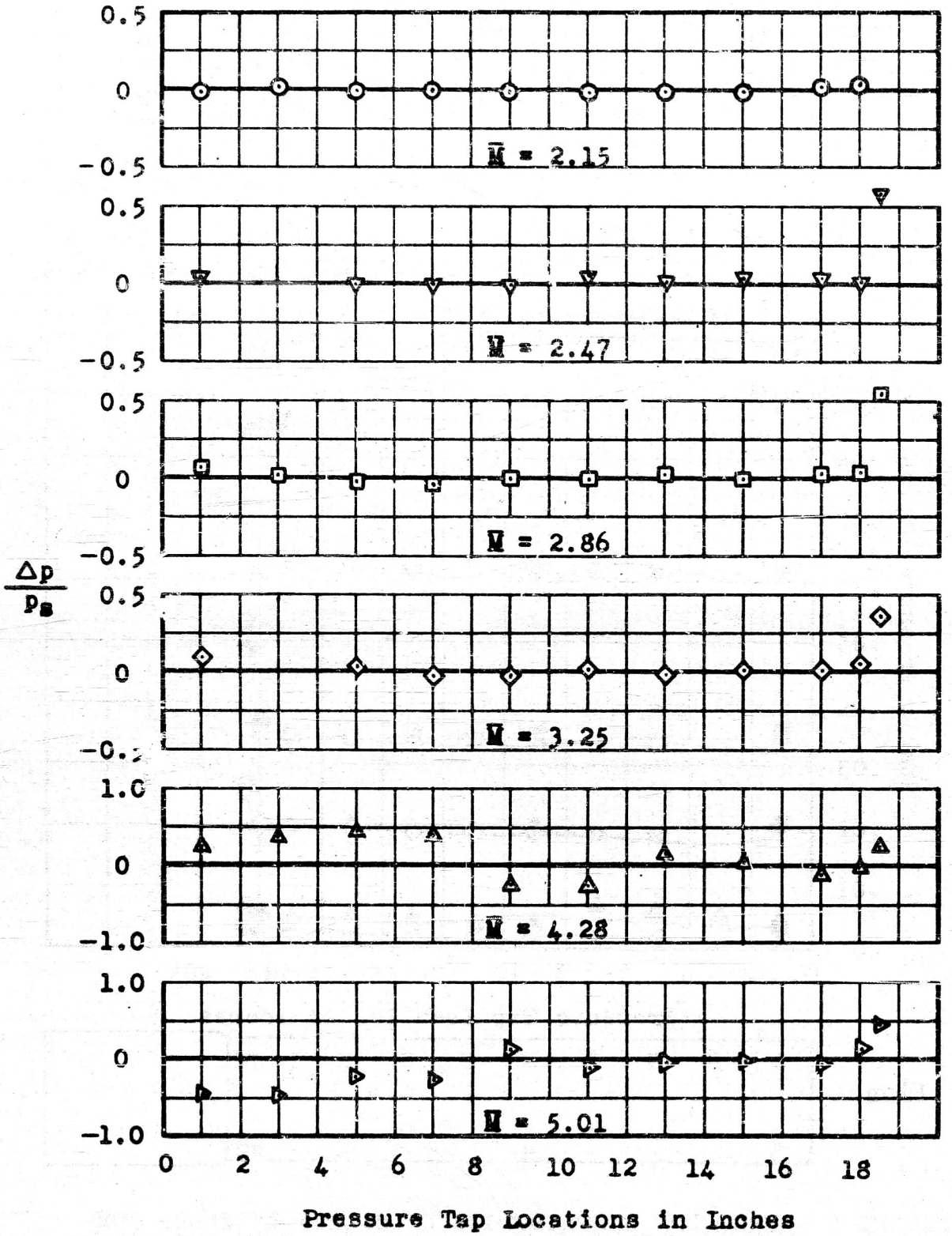

FIGURE 6 - PRESSURE DISTRIBUTION EXPRESSED BY $\Delta p/p_s$

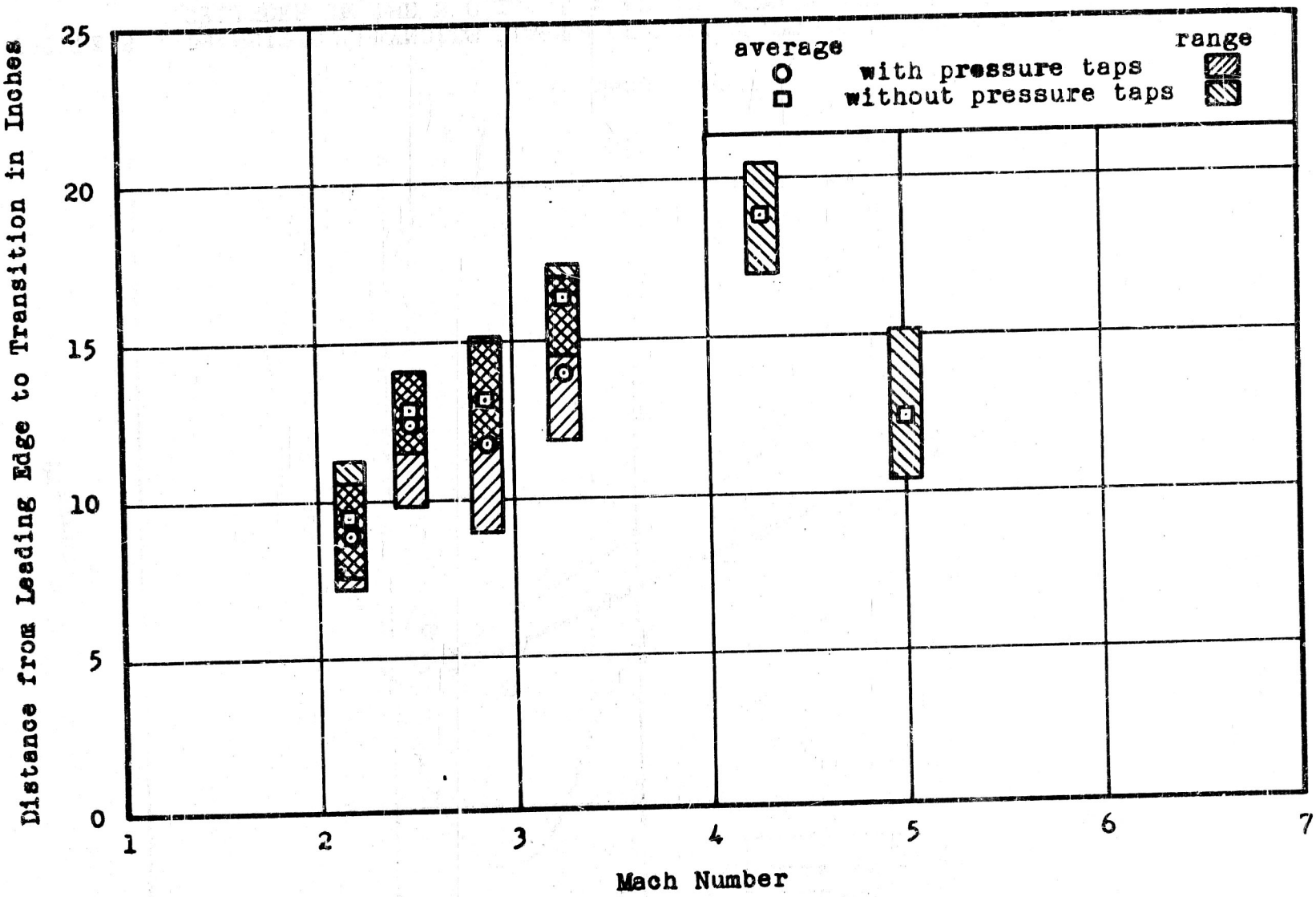

FIGURE 7 - LOCATION OF BOUNDARY LAYER TRANSITION ON HOLLOW CYLINDER

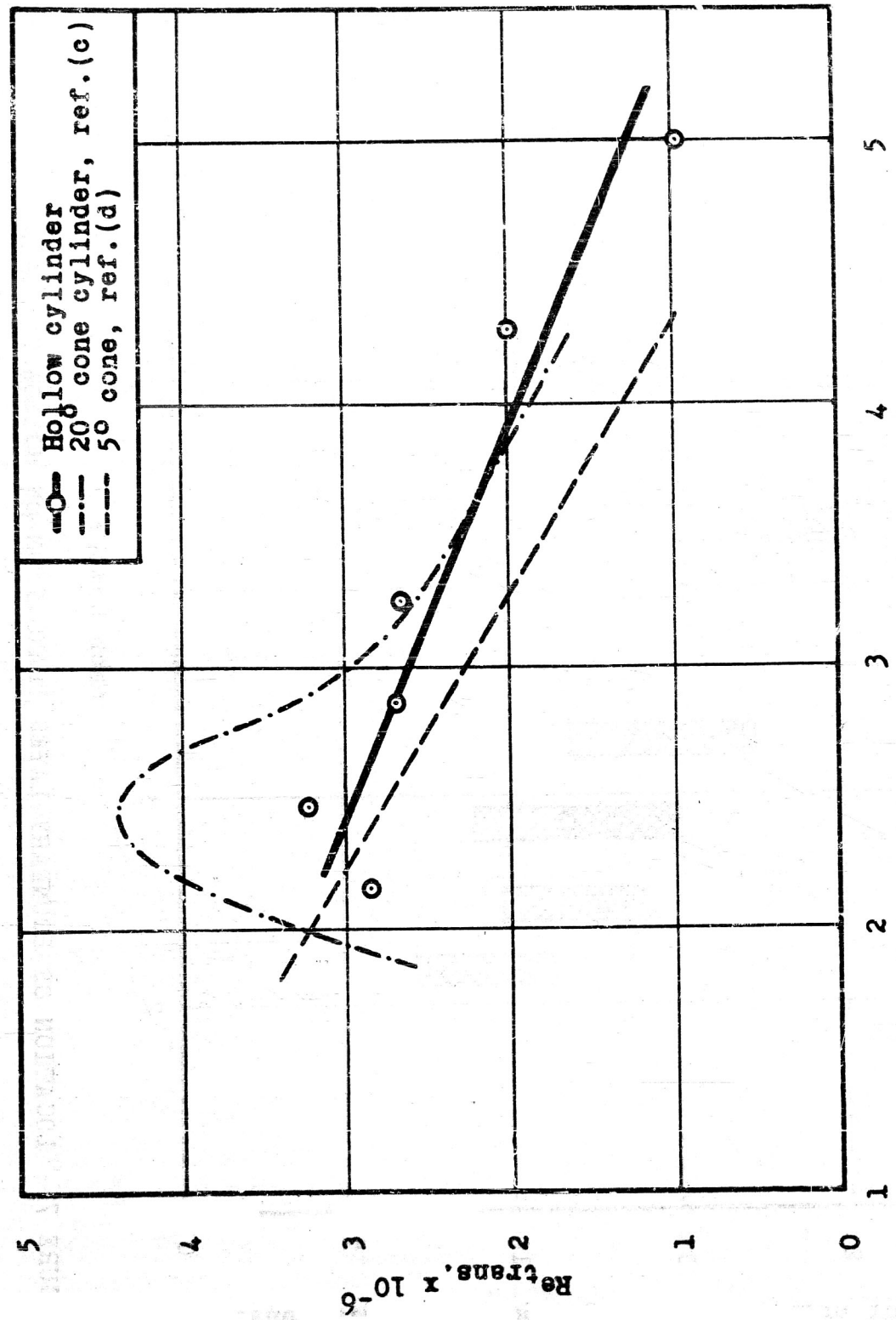

FIGURE 8 - TRANSITION REYNOLDS NUMBER OF HOLLOW CYLINDER, 5° CONE AND 20° CONE-CYLINDER IN THE N.O.L. 40 x 40 CM. WIND TUNNEL NO. 2

Aerobailistic Research Department
External Distribution List for Development (X2)

No. of Copies	
	Chief, Bureau of Ordnance Department of the Navy Washington 25, D. C.
1	Attn: Rea
1	Attn: Rexe
1	Attn: Re3d
3	Attn: Re9a
	Chief, Bureau of Aeronautics Department of the Navy Washington 25, D. C.
1	Attn: AER-TD-414
2	Attn: RS-7
	Commander U.S. Naval Ordnance Test Station Inyokern P.O. China Lake, California
2	Attn: Technical Library
	Commander U.S. Naval Air Missile Test Center Point Mugu, California
3	Attn: Technical Library
	Superintendent U.S. Naval Postgraduate School Monterey, California
1	Attn: Librarian
	Commanding Officer and Director David Taylor Model Basin Washington 7, D. C.
1	Attn: Hydrodynamics Laboratory
	Chief of Naval Research Navy Research Section Library of Congress
2	Washington 25, D. C.
	Chief, Naval Operations Department of the Navy Washington 25, D. C.
1	Attn: Op-51
	Office of Naval Research Department of the Navy Washington 25, D. C.
2	Attn: Code 463
	Director Naval Research Laboratory Washington 25, D. C.
1	Attn: Code 2021 Code 3800
	Officer-in-Charge Naval Aircraft Torpedo Unit U.S. Naval Air Station
1	Quonset Point, Rhode Island
	Office, Chief of Ordnance Washington 25, D. C.
1	Attn: ORDTU

No. of Copies	
	Research and Development Board Library Branch Pentagon 3D1041
2	Washington 25, D. C.
	Chief, AFSWP P.O. Box 2610 Washington, D. C.
1	Attn: Technical Library
	Chief, Physical Vulnerability Branch Air Targets Division Directorate of Intelligence Headquarters, USAF
1	Washington 25, D. C.
	The Artillery School Antiaircraft and Guided Missiles Br. Fort Bliss, Texas
2	Attn: Research and Analysis Sec.
	Commanding General Wright Air Development Center Wright-Patterson Air Force Base Dayton, Ohio
8	Attn: WCAPD
2	Attn: WCRR
1	Attn: WCSD
5	Attn: WCSO
	Director Air University Library
1	Maxwell Air Force Base, Alabama
	Commanding General Aberdeen Proving Ground Aberdeen, Maryland
1	Attn: C.L. Poor
	National Bureau of Standards Washington 25, D. C.
1	Attn: Librarian (Ord. Dev. Div.)
1	Attn: W. Ramberg
	National Bureau of Standards Corona Laboratories (Ord.Dev.Div.) Corona, California
1	Attn: Dr. H. Thomas
	National Bureau of Standards Building 3U, UCLA Campus 405 Hilgard Avenue Los Angeles 24, California
1	Attn: Librarian
	University of California Berkeley 4, California
1	Attn: Mr. G. J. Maslach
1	Attn: Dr. S. A. Schaaf
	California Inst. of Technology Pasadena 4, California
2	Attn: Librarian(Guggenheim Aero. Lab.) VIA: BuAero

No. of Copies

University of Michigan
Willow Run Research Center
Ypsilanti, Michigan
1 Attn: L.R. Biasell
VIA: InsMat

University of Minnesota
Rosemount, Minnesota
1 Attn: J. Leonard Frame
VIA: Ass't InsMat

The Ohio State University
Columbus, Ohio
1 Attn: G.L. VonEschen
VIA: Ass't InsMat

Polytechnic Institute of Brooklyn
99 Livingston Street
Brooklyn 2, New York
1 Attn: Dr. Antonio Ferri
VIA: ONR Branch Office

Princeton University
Forrestal Research Center Library
Project Squid
1 Princeton, New Jersey

Massachusetts Inst. of Technology
Project Meteor
Cambridge 39, Massachusetts
2 Attn: Guided Missiles Library

Applied Physics Laboratory
The Johns Hopkins University
8621 Georgia Avenue
Silver Spring, Maryland
1 Attn: Arthur G. Norris
Technical Reports Office
VIA: NIO

Armour Research Foundation
35 West 33rd Street
Chicago 16, Illinois
1 Attn: Engr. Mechanics Division
VIA: ONR Branch Office

Defense Research Laboratory
University of Texas
Box 1, University Station
1 Austin, Texas
VIA: InsMat

Eastman Kodak Company
Navy Ordnance Division
50 West Main Street
Rochester 4, New York
2 Attn: Dr. Herbert Trotter, Jr.
VIA: NIO

No. of Copies

General Electric Company
Building #1, Campbell Avenue Plant
Schenectady, New York
1 Attn: J.C. Hoffman
VIA InsMachinery

The Rand Corporation
1500 Fourth Street
Santa Monica, California
1 Attn: The Librarian
VIA InsMat

Consolidated Vultee Corporation
Daingerfield, Texas
1 Attn: J.E. Arnold, Manager
VIA: Dev. Contract Office

Douglas Aircraft Company, Inc.
3000 Ocean Park Boulevard
Santa Monica, California
1 Attn: Mr. E.F. Burton
VIA: BuAero Resident Rep.

North American Aviation, Inc.
12214 Lakewood Boulevard
Downey, California
2 Attn: Aerophysics Laboratory
VIA: BuAero Rep.

National Advisory Committee for Aero.
1724 F Street Northwest
Washington 25, D. C.
5 Attn: Mr. E. B. Jackson

Ames Aeronautical Laboratory
Moffett Field, California
1 Attn: H. Julian Allen
2 Attn: A.C. Charters

Theoretical Aerodynamics Division
Langley Aeronautical Laboratory
Langley Field, Virginia
1 Attn: Theoretical Aerodynamics Div.
1 Attn: Dr. A. Busemann
2 Attn: J. Steele

NACA Lewis Flight Propulsion Lab.
Cleveland Hopkins Airport
Cleveland, Ohio
1 Attn: Dr. John C. Evvard

Hughes Aircraft Company
Culver City, California
1 Attn: Dr. Allen E. Puckett

Institute of Aerophysics
University of Toronto
Toronto 5, Ontario
1 Attn: Dr Gordon N. Patterson, Dir.
VIA: BuOrd (Ad8)

Aeroballistic Research Department
External Distribution List for Applied Math. (X3a)

No. of Copies	
8	Office of Naval Research Branch Office, Navy 100 Fleet Post Office New York, New York
1	Commanding General Aberdeen Proving Ground Aberdeen, Maryland Attn: C.L. Poor
1	Attn: Dr. B.L. Hicks
1	National Bureau of Standards Washington 25, D. C. Attn: G.B. Schubauer
1	Ames Aeronautical Laboratory Moffett Field, California Attn: W.G. Vincenti
1	Brown University Providence 12, Rhode Island Attn: Prof. Wm. Prager VIA: Ass't InsMat
1	University of California Observatory 21 Berkeley 4, California Attn: Leland E. Cunningham VIA: InsMat
1	Cornell University Ithaca, New York Attn: W.R. Sears VIA: ONR
1	Indiana University Bloomington, Indiana Attn: T.Y. Thomas VIA: Ass't InsMat
1	Massachusetts Institute of Technology 77 Massachusetts Avenue Cambridge 39, Massachusetts Attn: Prof. Eric Reissner VIA: InsMat
1	Stanford University Stanford, California Attn: R.J. Langle VIA: Ass't InsMat
1	Case Institute of Technology Cleveland, Ohio Attn: Prof. G. Kuerti VIA: ONR
1	Harvard University 109 Pierce Hall Cambridge 38, Massachusetts Attn: Prof. R. von Mises

EXTERNAL DISTRIBUTION

	No. of Copies
Holloman Air Development Center Holloman Air Force Base, New Mexico Attn: Dr. G. R. Eber	1
Jet Propulsion Laboratory Pasadena, California Attn: Dr. P. P. Wegener	1
Redstone Arsenal Huntsville, Alabama Attn: Mr. J. L. Potter	1
NACA Lewis Flight Propulsion Laboratory Cleveland Hopkins Airport Cleveland, Ohio	
Attn: Dr. Ribner	1
Attn: Mr. Brinich	1